

Measuring Three Vector Boson Couplings in $qq \rightarrow qqW$ at the SSC *U. Baur¹ and D. Zeppenfeld²¹*Department of Physics, Florida State University, Tallahassee, FL 32306, USA*²*Department of Physics, University of Wisconsin, Madison, WI 53706, USA***ABSTRACT**

We investigate the electroweak process $qq \rightarrow qqW$, *i.e.* W production via $W\gamma$ and WZ fusion, as a probe for nonstandard $WW\gamma$ and WWZ vertices at hadron supercolliders. Triggering on events with one very forward and one very backward jet while requiring the W decay lepton to be central, strongly enhances the triple gauge boson vertex contribution and suppresses backgrounds from QCD Wjj events and $t\bar{t}j$ production below the signal level. At the SSC, the process is sensitive to WWV , $V = \gamma, Z$ couplings $\kappa_V - 1$, λ_V , and g_1^Z in the $0.03 \dots 0.1$ range.

1. Introduction

The study of electroweak processes is one of the main tasks of experiments at the SSC or the LHC. In order to probe the interactions in the bosonic sector of the Standard Model (SM) as completely as possible one would like to have available a large number of basic processes and correspondingly a large number of observables. This includes the search for the Higgs boson in both gluon fusion and weak boson fusion reactions in order to measure the Higgs couplings to known particles. Electroweak boson pair production ($q\bar{q} \rightarrow W\gamma$, WZ and W^+W^-) probes the non-abelian $WW\gamma$ and WWZ couplings. Quartic weak boson couplings are probed in elastic weak boson scattering and multiple weak boson production.

Here we report on investigations of a process which will be complementary to weak boson pair production in the measurement of the $WW\gamma$ and WWZ triple gauge boson vertices (TGV's), namely single W production via the electroweak process $qq \rightarrow qqW$ (to be called "signal" process in the following). Representative Feynman graphs are shown in Fig. 1.

It is via the first graph, the $W\gamma$ or WZ fusion contribution, that this process is sensitive to deviations of the TGV's from their SM predictions. While $W\gamma$, WZ , or W^+W^- production at hadron or e^+e^- colliders probe the TGV's for time-like momenta of all interacting electroweak bosons, the signal process measures these TGV's for space-like momentum transfer of two of the three gauge bosons and hence is complementary to the pair production processes.

*To appear in the Proceedings of the Workshop "Physics at Current Accelerators and the Supercollider", Argonne National Laboratory, June 2 – 5, 1993.

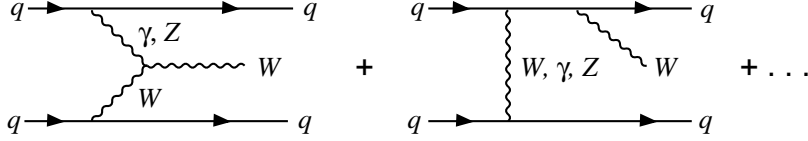


Fig. 1: Feynman graphs for the $qq \rightarrow qqW$ signal.

In the following we use the standard parameterization of the TGV's in terms of C and P conserving anomalous couplings g_1^V , κ_V and λ_V to quantify the sensitivity of the signal. These couplings can be defined by the effective Lagrangian¹

$$i\mathcal{L}_{eff}^{WWV} = g_{WWV} \left(g_1^V (W_{\mu\nu}^\dagger W^\mu - W^{\dagger\mu} W_{\mu\nu}) V^\nu + \kappa_V W_\mu^\dagger W_\nu V^{\mu\nu} + \frac{\lambda_V}{m_W^2} W_{\rho\mu}^\dagger W^\mu{}_\nu V^{\nu\rho} \right). \quad (1)$$

Here the overall coupling constants are defined as $g_{WW\gamma} = e$ and $g_{WWZ} = e \cot \theta_W$ where θ_W is the Weinberg angle. Within the SM, the couplings are given by $g_1^Z = g_1^\gamma = \kappa_Z = \kappa_\gamma = 1$, and $\lambda_Z = \lambda_\gamma = 0$. g_1^γ is just the electric charge of the W and hence fixed to 1 by electromagnetic gauge invariance. This leaves five couplings which need to be determined experimentally. Deviations of these TGV's from their SM values lead to amplitudes, e.g. for W pair production, which grow with energy, eventually violating partial wave unitarity.² Hence, anomalous TGV's must actually be form-factors, decreasing at large momentum transfer, a consideration which is essential at hadron supercolliders with their large available energy. Because of these form-factor effects the TGV's which can be measured at space-like momentum transfer in $qq \rightarrow qqW$ may in fact be different from the ones probed in vector boson pair production at space-like momenta.

2. Signal and Background Calculation

The signal and all background cross sections were calculated using parton level Monte Carlo programs. For the signal the program evaluates the tree level cross sections for the process $q_1 q_2 \rightarrow q_3 q_4 \ell \nu$, $\ell = e, \mu$ and all relevant crossing related processes. A more detailed discussion of the signal calculation is given in Ref. 3; our code is identical to the one used there. For the quark and gluon structure functions inside the proton we use set HMRS(B) of Harriman *et al.*⁴ for both signal and background processes.

Anticipating large backgrounds, all the features of the final state Wjj system need to be exploited for background suppression. Hence, we only consider the signal in the case when both final state (anti)quarks have transverse momenta larger than 40 GeV, allowing their identification as hadronic jets. Even though the resulting total cross section is sizable, $\sigma_{\text{sig}}(pp \rightarrow W^\pm jj) = 203$ pb at the SSC, one still needs to fight much larger backgrounds. They mainly arise from Drell-Yan production of W 's and from $t\bar{t}$ production with subsequent $t \rightarrow Wb$ decay.

The dominant background source is Drell-Yan production of W 's with an expected cross section of 100 to 300 nb⁵ at the SSC, 3 orders of magnitude larger than

the Wjj signal. The background cross sections including the additional two final state jets are calculated via the $\mathcal{O}(\alpha_s^2)$ real emission corrections to the Drell-Yan process. We use a parton level Monte Carlo program based on the work of Ref. 6 to model this “QCD Wjj ” background. The scales of the parton distribution functions and of the strong coupling constant $\alpha_s(Q^2)$ are chosen to be the transverse energy of the produced W . One may wonder whether double parton scattering (DPS) is an important source of background events. Here one pair of partons would yield a Wj final state and the second parton pair gives rise to a dijet system, supplying the second required jet. This question has been analyzed in Ref. 3 with the result that DPS is smaller than the QCD Wjj background by roughly one order of magnitude. Since we use acceptance cuts similar to the ones of Ref. 3 we expect the same relative suppression and we shall neglect the DPS background in the following.

$t\bar{t}$ production with subsequent $t \rightarrow Wb$ decay is another prominent source for W ’s. For a top-quark mass of $m_t = 140$ GeV the production cross section is $\sigma(pp \rightarrow t\bar{t}X) \approx 15$ nb⁷ and hence about two orders of magnitude larger than the Wjj signal. A characteristic feature of the W signal is the presence of two energetic forward jets. In Ref. 8 it was shown in connection with single forward jet tagging that the dominant source of forward jets in $t\bar{t}$ events arises from QCD radiation, *i.e.* the additional parton in $t\bar{t}j$ events, and not from the top decay products. Hence we model the top background with a tree level Monte Carlo program based on the matrix elements of Ref. 9 for the processes $pp \rightarrow t\bar{t}j \rightarrow W^+bW^-\bar{b}j$. A phase space distribution is assumed for the subsequent $t \rightarrow Wb$ and $W \rightarrow \ell\nu, q\bar{q}'$ decays. While the top background analysis is performed with a top quark mass of 140 GeV, we have checked that a mass as light as 110 GeV does not change the top background level qualitatively.

3. Acceptance Cuts and Background Suppression

In order to gain good sensitivity to the TGV we need to identify the phase space region in which the electroweak boson fusion graph of Fig. 1 is important. Clearly this graph is enhanced at small Q^2 of the incident γ, Z and W , of order m_W^2 or less. These virtualities are much smaller than the typical lab frame energies of the scattering quarks which, therefore, emerge at very small angles. Hence we want to tag events with one very forward and one very backward jet (arising from the spectator quark jets), while the lepton originating from the $W \rightarrow \ell\nu$ decay is to be expected in the central region.

A search algorithm for the signal events has been outlined in Ref. 3, emphasizing the “rapidity gap” characteristics of the signal. We closely follow this approach for the lepton and jet acceptance cuts but do not require low hadronic activity in the central region. Events are triggered by a charged lepton of transverse momentum

$$p_{T\ell} > 20 \text{ GeV} , \quad (2)$$

and we require missing transverse momentum in excess of 50 GeV as a signature for W leptonic decays. On either side of the charged lepton (with respect to pseudorapidity) one then searches for the first hadronic jet with

$$p_{Tj} > 40 \text{ GeV} , \quad |\eta_j| < 5 , \quad (3)$$

which will be called tagging jets and represent the two spectator quarks in our signal calculation. Leptons and jets are required to be well separated

$$R_{jj} = (\Delta\eta_{jj}^2 + \Delta\phi_{jj}^2)^{\frac{1}{2}} > 0.7, \quad R_{\ell j} = (\Delta\eta_{\ell j}^2 + \Delta\phi_{\ell j}^2)^{\frac{1}{2}} > 0.7. \quad (4)$$

The forward-backward nature of the two tagging jets is then taken into account by requiring

$$-5 < \eta_{j1} < -2.5, \quad 2.5 < \eta_{j2} < 5. \quad (5)$$

Notice that this implies the existence of a central “rapidity gap”, at least 5 units wide in pseudorapidity, which contains the charged lepton but no jets with $p_T > 40$ GeV.

The above requirements leave a QCD Wjj background which is about a factor six larger than the remaining signal. However, the background is dominated by W -bremsstrahlung off initial or final state quarks, a class of events which is also present in the electroweak signal and obscures the contribution from the electroweak boson fusion graph. W -bremsstrahlung and electroweak boson fusion lead to drastically different lepton pseudorapidity distributions for the signal and the QCD background.

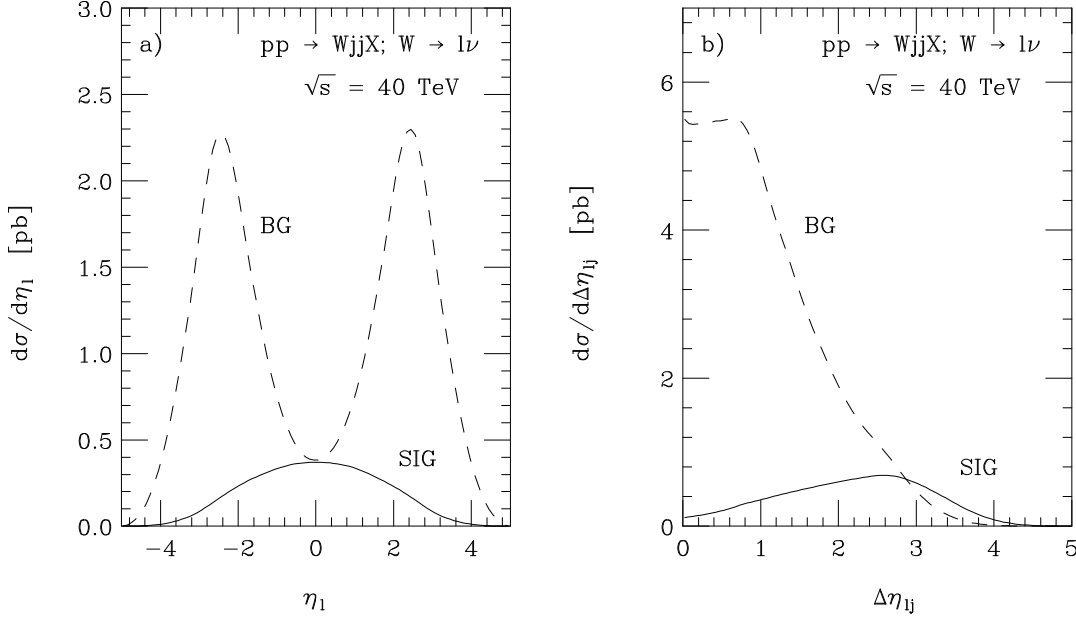


Fig. 2: a) Pseudorapidity distribution $d\sigma/d\eta_\ell$ of the charged decay lepton in Wjj , $W \rightarrow \ell\nu$ events at the SSC. b) Minimum separation in pseudorapidity of the decay lepton from the two tagging jets. Distributions are given for the signal (solid lines) and the QCD background (dashed lines).

Shown in Fig. 2a is the η_ℓ distribution of the charged lepton. W -bremsstrahlung emits the W 's and hence also the decay leptons either close to the beam pipe or close to the tagging jets, which are also required to be very forward. As a result central lepton rapidities are rare for the QCD background if the jet tagging cuts of Eq. 5 are imposed, while weak boson fusion favors central leptons. Closely related are the distributions of

Fig. 2b which show the smallest separation of the decay lepton from the two tagging jets. Again the dominance of W -bremsstrahlung in the QCD background is evident. It is strongly suppressed by requiring

$$|\eta_\ell| < 1.5, \quad \Delta\eta_{\ell j} = \min(|\eta_\ell - \eta_{j_1}|, |\eta_\ell - \eta_{j_2}|) > 2.5, \quad (6)$$

and already leads to a signal slightly larger than the QCD background (620 fb vs. 500 fb).

A further strong background rejection is achieved by exploiting the very large dijet invariant masses which are typical for the vector boson fusion process. The m_{jj} -distributions (after imposing the cuts of Eq. 6) are shown in Fig. 3.

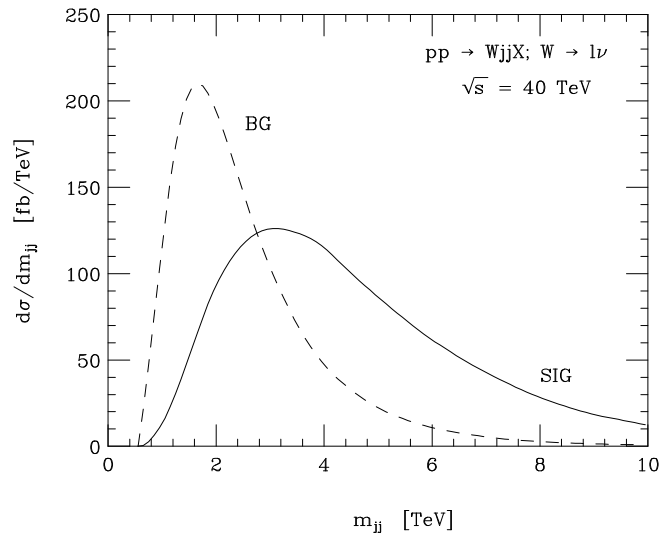


Fig. 3: Invariant mass distribution of the two tagging jets for the signal (solid line) and the QCD background (dashed line) at the SSC.

A dijet invariant mass cut of

$$m_{jj} > 3 \text{ TeV}, \quad (7)$$

imposed on the two tagging jets, reduces the background well below signal level ($\sigma_{\text{SIG}} = 450 \text{ fb}$ vs. $\sigma_{\text{QCD}} = 136 \text{ fb}$ for the QCD Wjj background and $\sigma_{t\bar{t}j} = 38 \text{ fb}$ for the top-quark background at $m_t = 140 \text{ GeV}$).

4. Sensitivity to the WWV Vertex

The cuts discussed in the previous section single out the phase space region in which the electroweak fusion process dominates and hence we expect a pronounced sensitivity to deviations in the TGV's from the SM prediction. Because of the extra derivatives in the operators of the effective Lagrangian of Eq. 1 and the now incomplete gauge theory cancelations for longitudinal polarization of the incoming gauge bosons, anomalous coupling effects are enhanced at large momentum transfer and, hence, for

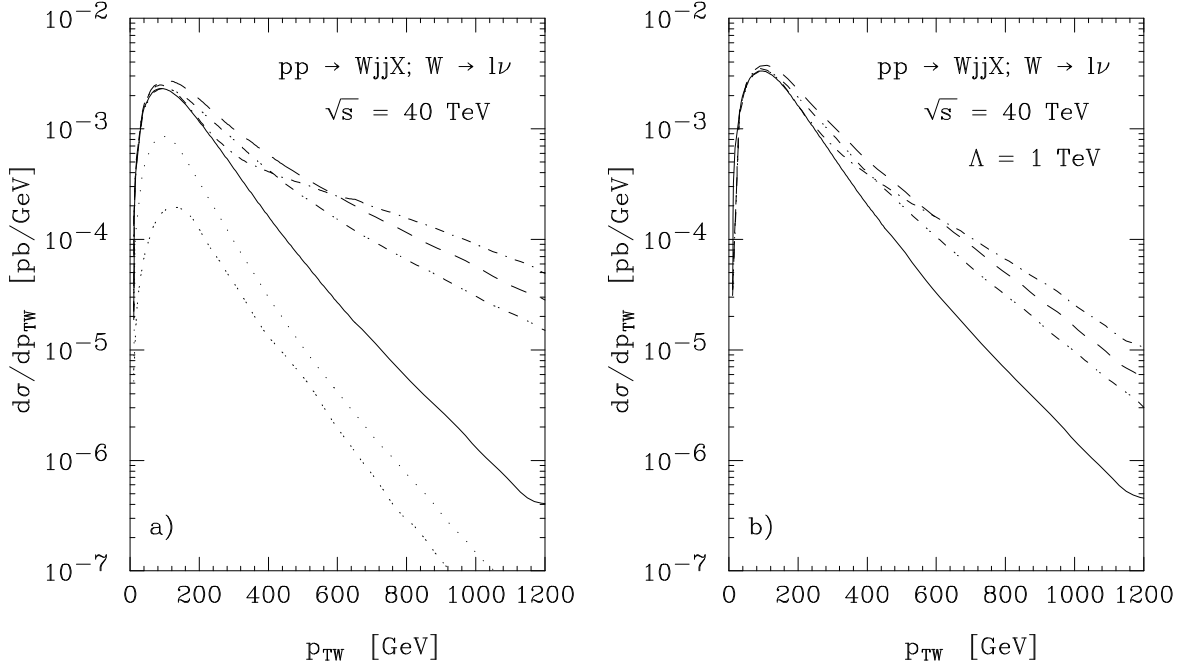


Fig. 4: Transverse momentum distribution of the produced W -boson in Wjj events at the SSC. Part a) shows individual distributions for the SM signal (solid line) the QCD Wjj background (dotted line) and the $t\bar{t}j$ background for $m_t = 140$ GeV (double dotted line). The upper three curves correspond to three choices of anomalous couplings: $\kappa_\gamma = \kappa_Z = 1.2$ (dashed line) $\lambda_\gamma = \lambda_Z = 0.1$ (dash-dotted curve) and $g_1^Z = 1.2$ (dash-double dotted line). In part b) the two background distributions have been added to the four signal curves. In addition the effect of the form-factor of Eq. 8 is shown for a scale $\Lambda = 1$ TeV. The cuts imposed are described in the text.

large transverse momenta of the produced W -boson. The effect is demonstrated in Fig. 4. While the p_{TW} distributions show similar shapes for the SM signal and the QCD and top quark backgrounds, a strong enhancement at large transverse momenta arises from anomalous couplings like $\kappa_\gamma - 1 = \kappa_Z - 1 = 0.2$ (dashed line) $\lambda_\gamma = \lambda_Z = 0.1$ (dash-dotted curve) and $g_1^Z - 1 = 0.2$ (dash-double dotted line). For these three curves all other anomalous couplings are set to zero. We actually find the p_{TW} distribution to be the one which is the single most sensitive to anomalous TGV's. The dotted and double dotted curves in Fig. 4a represent the QCD Wjj and the $t\bar{t}j$ background (with $m_t = 140$ GeV), respectively. For a smaller top quark mass of $m_t = 110$ GeV, the p_{TW} differential cross section from $t\bar{t}j$ production is enhanced by roughly a factor two in the peak region around $p_{TW} \approx 100$ GeV. For W transverse momenta larger than 400 GeV, where deviations from the SM are most pronounced, there is only little variation of the differential cross section with m_t .

The anomalous couplings used in Fig. 4a are of the same order or below the sensitivity limits expected for W^+W^- production at LEP II.¹⁰ However, at LEP II these couplings are probed at relatively small time-like momentum transfers of order

Table 1: Sensitivities achievable at the 2σ level for the anomalous WWV , $V = \gamma, Z$ couplings $\Delta\kappa_V = \kappa_V - 1$, λ_V , and $\Delta g_1^Z = g_1^Z - 1$ in $pp \rightarrow W^\pm jj \rightarrow \ell^\pm \nu jj$ at the SSC. Only one coupling at a time is varied. We assume an integrated luminosity of 10 fb^{-1} . The cuts imposed and the form-factor ansatz used are described in the text. The limits are displayed for form-factor scales of $\Lambda = 1 \text{ TeV}$ and $\Lambda = \infty$.

coupling	$\Lambda = 1 \text{ TeV}$	$\Lambda = \infty$	coupling	$\Lambda = 1 \text{ TeV}$	$\Lambda = \infty$
$\Delta\kappa_\gamma$	+0.09 −0.18	+0.06 −0.11	$\Delta\kappa_Z$	+0.05 −0.09	+0.04 −0.05
λ_γ	+0.05 −0.05	+0.03 −0.03	λ_Z	+0.03 −0.03	+0.02 −0.02
Δg_1^γ	—	—	Δg_1^Z	+0.05 −0.11	+0.03 −0.06

$q^2 = (200 \text{ GeV})^2$, while the single W production process is most sensitive at large space-like momentum transfers of order $-q^2 \approx p_{TW}^2 = (1 \text{ TeV})^2$. These different scales raise the possibility that form-factor effects may be important in the Wjj production considered here. We have shown previously¹¹ that anomalous couplings as large as the ones used in Fig. 4 do require form-factor damping for a momentum transfer above $|q| = 2 \text{ TeV}$ in order not to violate partial wave unitarity in vector boson pair production. By analytic continuation we expect a similar form-factor scale also in the space-like region.

In Fig. 4b we show results including such form-factor effects. We have replaced the anomalous TGV's $a = \kappa_V - 1$, $g_1^Z - 1$, or λ_V by

$$a \rightarrow \frac{a}{(1 + |q_1^2|/\Lambda^2)(1 + |q_2^2|/\Lambda^2)(1 + |q_3^2|/\Lambda^2)} , \quad (8)$$

with a cutoff scale $\Lambda = 1 \text{ TeV}$. Here q_1 , q_2 , and q_3 denote the four-vectors of the three vector bosons entering the TGV in Fig. 1.

Form-factor effects are clearly important in the measurement of TGV's at the SSC; the very large enhancements above $p_{TW} = 1 \text{ TeV}$ in Fig. 4a are most likely unrealistic and the situation in Fig. 4b represents a more likely scenario. Nevertheless, $qq \rightarrow qqW$ production is a sensitive probe for anomalous couplings. In the region above $p_{TW} = 400 \text{ GeV}$ the anomalous coupling curves in Fig. 4b correspond to an expected rate of 600–800 $W \rightarrow e\nu$, $\mu\nu$ events per SSC year (10 fb^{-1}) as compared to about 200 events for the SM.

The results of a more quantitative analysis of the sensitivity of Wjj production to anomalous TGV's are shown in Table 1 where we list the 2σ limits achievable for $\Lambda = 1 \text{ TeV}$ at the SSC. Only one coupling at a time is assumed to differ from its SM value. In order to demonstrate the effect of the form-factor behavior of the anomalous couplings, we also display sensitivity bounds for $\Lambda = \infty$, which is equivalent to ignoring the momentum dependence of the non-standard WWV couplings. We calculate the statistical significance by splitting the p_{TW} distribution into 12 bins, 11 of

which are 60 GeV wide. In each bin the Poisson statistics is approximated by a Gaussian distribution. In order to achieve a sizable counting rate in each bin, all events with $p_{TW} > 660$ GeV are collected in one bin. To derive realistic limits we allow for a normalization uncertainty of 50% in the SM cross section. The QCD Wjj and $t\bar{t}j$ background contributions are fully incorporated in our procedure.

The results collected in Table 1 indicate that the WWV vertices can be probed in $qq \rightarrow qqW$ at the few percent level in general. Form-factor effects may weaken the achievable bounds by up to a factor 1.5, for form-factor scales above 1 TeV. Comparing our results with those obtained in Ref. 12, we find that the process $qq \rightarrow qqW$ is significantly more sensitive to $\Delta\kappa_V$ and Δg_1^Z than $W\gamma$ and WZ production for cutoff scales Λ in the low TeV range. The measurement of λ_V is competitive. In general, the pair production process is affected more by details of the form-factors, which in addition may be quite different in the space-like and the time-like regions. This emphasizes the need to measure pair production and Wjj production if full information on the WWV couplings is to be gained.

Acknowledgements

This research was supported in part by the University of Wisconsin Research Committee with funds granted by the Wisconsin Alumni Research Foundation, by the U. S. Department of Energy under contracts No. DE-AC02-76ER00881 and DE-FG05-87ER40319, and by the Texas National Research Laboratory Commission under Grants No. RGFY9273 and FCFY9212.

References

1. K. Hagiwara, *et al.*, Nucl. Phys. **B282** (1987) 253.
2. J. M. Cornwall, *et al.*, Phys. Rev. Lett. **30** (1973) 1268, Phys. Rev. **D10** (1974) 1145; C. H. Llewellyn Smith, Phys. Lett. **46B** (1973) 233; S. D. Joglekar, Ann. Phys. **83** (1974) 427.
3. H. Chehime and D. Zeppenfeld, Phys. Rev. **D47** (1993) 3898.
4. P. N. Harriman, *et al.*, Phys. Rev. **D42** (1990) 798.
5. H. Kuijf *et al.*, *Proceedings of the ECFA Large Hadron Collider Workshop*, October 4–9, 1990, Aachen, Germany, G. Jarlskog and D. Rein eds., CERN 90-10, Vol. II, p. 91.
6. K. Hagiwara and D. Zeppenfeld, Nucl. Phys. **B313** (1989) 560; V. Barger, T. Han, J. Ohnemus, and D. Zeppenfeld, Phys. Rev. **D40** (1989) 2888.
7. D. Denegri, *Proceedings of the ECFA Large Hadron Collider Workshop*, October 4–9, 1990, Aachen, Germany, G. Jarlskog and D. Rein eds., CERN 90-10, Vol. I, p. 56.
8. V. Barger *et al.*, Phys. Rev. **D44** (1991) 2701 and MAD/PH/757 (preprint, May 1993).
9. R. K. Ellis and J. C. Sexton, Nucl. Phys. **B282** (1987) 642.
10. M. Bilenky *et al.*, BI-TP 92/44 (preprint, February 1993).
11. U. Baur and D. Zeppenfeld, Phys. Lett. **B201** (1988) 383.

12. U. Baur and D. Zeppenfeld, Nucl. Phys. **B308** (1988) 127; U. Baur *et al.*, FSU-HEP-930519, to appear in Phys. Rev. **D**; S. Willenbrock and D. Zeppenfeld, Phys. Rev. **D37** (1988) 1775.